ELSEVIER

Thin Solid Films 353 (1999) 93–99

thin solid films

www.elsevier.nl/locate/tsf

Simultaneous determination of the optical properties and of the structure of r.f.-sputtered ZnO thin films

E. Dumont*, B. Dugnoille, S. Bienfait

Service Science des Matériaux, Faculté Polytechnique de Mons, rue de l'Epargne 56, 7000 Mons, Belgium

Received 6 October 1998; received in revised form 1 June 1999; accepted 7 June 1999

Abstract

Thin films of zinc oxide were deposited on glass by r.f. sputtering and studied by means of spectrophotometry and spectroscopic ellipsometry. We first reviewed the methods used to determine simultaneously the microstructure and optical indices of thin films. These methods have then been used to analyze the experimental measurements. They clearly showed that the microstructure of thin films could only be determined by using spectroscopic ellipsometry measurements. From these measurements, the optical indices of the zinc oxide films in the wavelength range 310–750 nm were then computed. These correlate closely with previously published results.

Keywords: Ellipsometry; Optical properties; Structural properties; Zinc oxide

1. Introduction

For many years thin films made from transparent and conducting materials have attracted much attention because of their numerous applications, e.g. as transparent electrodes in optoelectronic devices [1,2], as heat mirrors [1,3] for energy saving, and in solar cells [1,4]. These materials are $In_2O_3SnO_2$ (ITO), SnO_2, ZnO and Cd_2SnO_4 [1]. They all have a band gap higher than 3 eV, allowing a high transmittance (above 80%) in the visible range, and a high carrier concentration giving a relatively high electrical conductivity (above $10^4\ \Omega^{-1}\ cm^{-1}$). The carrier concentration can be modified through control of the material stoichiometry or its doping with various elements. Research has mainly been carried out on ITO and SnO_2.

Zinc oxide is gaining more and more interest because of its low cost, non-toxicity, high band gap and ease of doping. These properties are used to produce thin films with optical and electrical properties similar to those of ITO films. This interest is increased by its piezo-electrical properties used in surface acoustic wave devices [5].

The most common deposition technique for ZnO thin films is sputtering [6–9]. Other techniques such as pulsed laser [10], aqueous route [11], chemical vapor deposition (CVD) [12] and pyrolytic spray [13] are also used. The making of ZnO layers by sputtering depends on various parameters. The influence of some of these on the properties of the final films have been examined: oxygen partial pressure [14], r.f. power [15], magnetron magnetic field intensity [16] and nature of the substrate [17]. The properties also depend on the post-deposition anneal [8,18]. All of these studies have focused mainly on the electrical properties of ZnO and much less on its optical properties. As a conducting and transparent material, the optical properties of ZnO are of great importance for numerous applications.

Many studies have shown that optical indices computed from experimental measurements on thin films in the UV-visible wavelength range depend on microstructure of the films [19]. Therefore, the optical indices of ZnO thin films were determined simultaneously with their microstructure. The experimental procedure is detailed in Section 2. In Section 3, the various methods used to determine the optical indices and microstructure of a thin film are reviewed. In Section 4, these methods are used for the analysis of the optical measurements. In Section 5, the methods are discussed and the computed optical indices are compared with previously published results.

2. Experimental

ZnO thin films were deposited on Corning 7059 glass plates by r.f. sputtering. The ZnO target was made with dehydrated ZnO powder (purity >99.999%), pressed and sintered for 1 h at 800°C. Thin films were made at a pressure

* Corresponding author. Tel.: +32-6537-4428; fax: +32-6537-4421.
E-mail address: dumonte@fpms.ac.be (E. Dumont)

0040-6090/99/$ - see front matter
PII: S0040-6090(99)00382-X

of 10^{-2} Torr with a mixture of 70% Argon and 30% Oxygen for 150 min. The sputtering power was 400 W and the substrate temperature was 20°C. The deposition rate was about 2.5 nm/min.

X-ray diffraction analysis has been carried out on the samples with a Siemens D5000 diffractometer. All the samples have the same diffraction spectrum. ZnO has the structure of wurtzite. When deposited on a glass substrate, its *c*-axis tends to be perpendicular to the substrate plane. This explains the presence of a single peak on the diffraction spectrum which corresponds to the ⟨002⟩orientation.

The microstructure and optical indices of the layers were determined by using ellipsometry and spectrophotometry. Ellipsometric measurements were taken on a customized Rudolph Research S2000 spectroscopic ellipsometer. This ellipsometer is of rotating polariser type with a fixed polariser and a fixed analyser. This configuration has been described elsewhere [20]. With the use of a compensator, it can give more accurate values of (Δ,Ψ) than standard RAE or RPE ellipsometers [19]. It also allows the measurement of the degree of polarisation *P* [21]. The measurements were taken in the wavelength range 310–750 nm. Reflectance (*R*) and transmittance (*T*) spectra were measured with a Perkin–Elmer λ19 spectrophotometer equipped with an integration sphere (Labsphere RSA-PE-19) in the range 250–2000 nm.

3. Theory

Several methods have been published for more than twenty years for the simultaneous determination of the microstructure and of optical indices of a thin film. They use spectrophotometric or spectroscopic ellipsometry measurements and need the definition of an optical model of the film. All these methods can be divided into two categories: direct computation methods and indirect computation methods.

3.1. Direct computation methods

Direct computation methods are used for the straightforward determination of the optical indices and microstructure of thin films from experimental measurements. For spectrophotometric measurements, Manifacier et al. [22] and Swanepoel [23] have published methods that assume the thin film to be flat, homogeneous and isotropic, characterized only by its thickness d_F (F ≡ Film). The film has a complex optical index $N_F(\lambda) = n_F(\lambda) - jk_F(\lambda)$, and is placed in an ambient medium with an index $N_A(\lambda) = n_A(\lambda) - jk_A(\lambda)$ (A ≡ Ambient) and deposited on a substrate with an index $N_S(\lambda) = n_S(\lambda) - jk_S(\lambda)$ (S ≡ Substrate). The indices vary with the wavelength λ. These methods use the extrema of either the reflectance *R* or transmittance *T* spectrum to compute the thickness d_F and the optical indices N_F of the film. Borgogno et al. has also published a method used for films having a linear variation in their optical indices [24]. For ellipsometric measurements, direct computation methods are not used except in very few cases described by Azzam and Bashara [25], which also assume the film to be flat, homogeneous and isotropic.

We used the method described by Swanepoel [23] to compute the thickness d_F and the optical indices $N_F(\lambda)$ of the ZnO thin film. This method uses the normal transmittance spectrum $T(\lambda)$ of the film.

3.2. Indirect computation methods

When the microstructure of the film is complex, e.g. when the film is rough, when there is an interface between the substrate and the film, or when the film is optically inhomogeneous, the optical model of the film has many parameters. These numerous parameters and the optical indices of the film can only be determined by using an indirect computation method. In these methods, the parameters are determined by minimizing the difference between the theoretical results of the optical model and the experimental measurements. Indirect computation methods are standard procedures for the analysis of spectroscopic ellipsometry measurements [26].

Spectroscopic ellipsometry gives two independent experimental values: Δ_{exp} and Ψ_{exp}, which are functions of wavelength λ and angle of incidence AI [26]. Δ_{th} and Ψ_{th} are computed values based on the optical model.

Determination of parameters uses a biased estimator, the reduced χ^2, to be minimised [26]

$$\chi^2 = \sum_{l=1}^{n} \frac{1}{n - n_x - 1}\left[\left(\frac{\Delta_{l\exp} - \Delta_{lth}}{\varepsilon\Delta_l}\right)^2 + \left(\frac{\Psi_{l\exp} - \Psi_{lth}}{\varepsilon\Psi_l}\right)^2\right] \quad (1)$$

where *n* is the number of measurements, n_x the number of parameters to be determined, $\varepsilon\Delta_l$ and $\varepsilon\Psi_l$ the experimental errors in $\Delta_{l\,exp}$ and $\Psi_{l\,exp}$. Minimization is performed using a modified version of the standard Levenberg–Marquardt algorithm [27]. For spectrophotometric measurements (*R*,*T*), this method can also be used, Δ and Ψ being replaced by *R* and *T* in Eq. (1).

In order to determine the microstructure parameters and optical indices of the thin film simultaneously, a model which decorrelates the optical indices from the structure parameters must be used. Two methods are generally used and are well described in the litterature [28]. In the first method, decorrelation is obtained by using optical measurements taken on several samples made of the same material but with different thicknesses. With this multiple sample analysis, the optical indices of the film $N_F(\lambda) = n_F(\lambda) - jk_F(\lambda)$ can be computed for each experimental wavelength λ. The second method uses a dispersion law and only needs optical measurements taken on one sample.

As our ZnO samples are transparent for wavelengths above 500 nm, we used the second method with a Sellmeier dispersion law. Although several parametric dispersion laws of $n_F(\lambda)$ and $k_F(\lambda)$ exist (e.g. Tauc–Lorentz [26,29,30]),

only a Sellmeier dispersion law has proved to be able to accurately model the spectral evolution of $n_F(\lambda)$ for a transparent material with a minimal number of parameters [31]

$$n_F^2(\lambda) = 1 + \frac{A\lambda^2}{\lambda^2 - B^2} \quad (2)$$

where A and B are the Sellmeier parameters.

The analysis of the experimental ellipsometric measurements was therefore performed in two parts:

1. in the range 500–750 nm, the structure parameters and the Sellmeier parameters of the layer are determined simultaneously;
2. in the range 310–500 nm, the structure being known, the values of $n_F(\lambda)$ and $k_F(\lambda)$ are computed for each experimental wavelength λ.

In this study, we assumed that the cause of inhomogeneity of thin films is a depth variation in the density of the layer, that is a depth variation of the ZnO volume fraction, F_v, in the layer. The F_v profile in the actual layer can be modelled by replacing it with a stack of flat homogeneous sublayers, every sublayer i having a constant volume fraction F_{vi} (graded model). The variation of the volume fraction from one sublayer to another follows the F_v profile of the actual layer. The index of each sublayer $N_{fi}(\lambda)$ (i for the ith sublayer) can be evaluated with the Bruggeman effective medium approximation (EMA) [32] for a mixture of compact ZnO and void, with a volume fraction of ZnO F_{vi}.

The interfaces of a film can also exhibit roughness. This roughness can be modelled by a layer having a thickness d_R (R ≡ Roughness) and composed of a 50% mixture of materials located on both sides of the interface [33]. The optical index of this layer is also computed using the Bruggeman EMA.

The parameters of the optical model of the thin film are the thicknesses d_{Fi} of each sublayer of the stack, the thickness of the rough layer d_R, the volume fractions F_{Vi} of each sublayer of the stack and the ZnO index $N_F(\lambda)$. These structure parameters were determined using several optical models of increasing complexity. As the value of the degree of polarization P lies between 0.995 and 1.002 for all wavelengths, the most common cause of depolarisation, thickness inhomogeneity [21], can be excluded. Many models have been used to fit the experimental data. Four basic models are described here (Fig. 1) and are listed with increasing complexity and best fit:

1. a transparent homogeneous layer. The parameters are A, B (Sellmeier) and layer thickness d_F;
2. a transparent homogeneous layer with a roughness layer of thickness d_R between the layer and the ambient medium. The parameters are A, B (Sellmeier), layer thickness d_F and roughness thickness d_R;
3. a transparent inhomogeneous layer for which the volume fraction of ZnO varies from 100% at the substrate-layer interface to F_V% at the ambient-layer interface. The volume fraction is assumed to be linear along with thickness of the layer (graded layer). The parameters are A, B (Sellmeier), layer thickness d_F and volume fraction F_V;
4. a transparent inhomogeneous layer with a roughness layer (combination of models 2 and 3). The parameters are A, B (Sellmeier), layer thickness d_F, roughness thickness d_R and volume fraction F_V.

4. Results

Optical measurements analysis has been done on a typical ZnO sample. The results of this analysis are presented below.

4.1. Direct computation methods

The typical transmittance spectrum of the ZnO thin film $T(\lambda)$ is shown in Fig. 2. The thickness of the layer determined from the successive interference minima and maxima is 342.5 ± 10.3 nm. The optical indices are presented in Fig. 4.

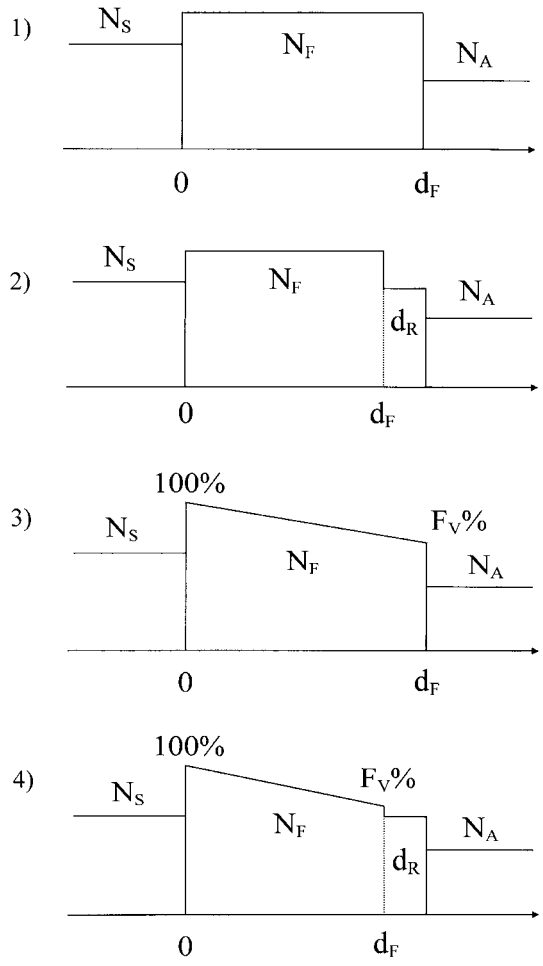

Fig. 1. Index profile definition for the four models described in the text.

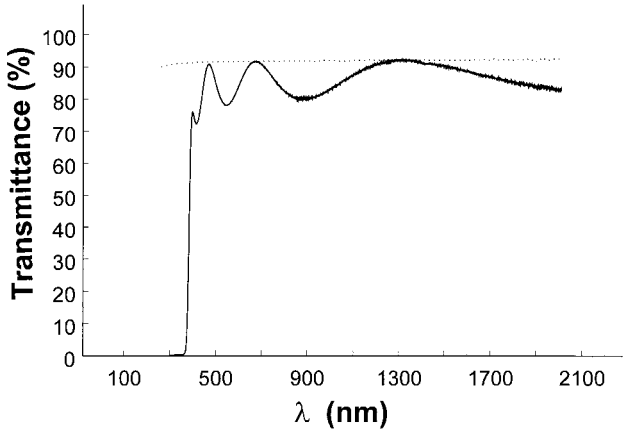

Fig. 2. Transmittance spectrum of a typical ZnO sample: (——), sample; (····) Corning 7059.

4.2. Indirect computation methods

Indirect computation has been first performed with the spectroscopic ellipsometry measurements and then with the spectrophotometric measurements. Spectrophotometric measurements were taken at an angle of 0° for T and of 8° for R. Ellipsometric measurements were performed at two angles: 60° and 70°. For comparison, the same range (500–750 nm) was used to determine the structure parameters from the spectrophotometric and ellipsometric measurements. The value of the parameters after minimisation of χ^2 is presented in Table 1.

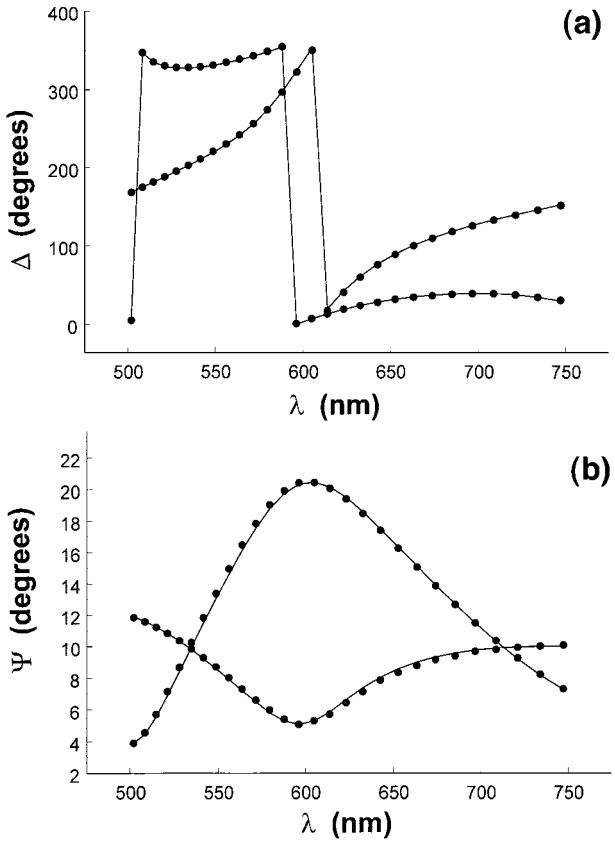

Fig. 3. Ellipsometric curves of the ZnO sample: (●), measurements; (——), fit of the best model (model 4).

5. Discussion

5.1. Thin film structure

The best optical model for the ZnO thin film must have the lowest χ^2 value. For every model, the cross-correlation matrix showed a low correlation between the fitted parameters. We can see from Table 1 that the four models have very different χ^2 values for the fit with ellipsometric measurements but not for the fit with spectrophotometric measurements. This is an experimental demonstration that ellipsometry is highly sensitive to microstructure parameters while spectrophotometry is less sensitive. The best model is an inhomogeneous film with upper roughness (model 4). The comparison between experimental results and theory is presented in Fig. 3. We can also observe that for the best model, the parameters have the same values for the fit with ellipsometric measurements and for the fit

Table 1
Results of the fit for the ZnO sample

Model	χ^2	Parameter values				
		A	B (μm)	d_F (nm)	d_R(nm)	F_V (%)
Results obtained from spectrophotometric measurements						
1	83	2.456 ± 0.003	0.206 ± 0.001	349.6 ± 0.1	–	–
2	56	2.548 ± 0.005	0.197 ± 0.001	340.9 ± 0.3	13.6 ± 0.3	–
3	50	2.499 ± 0.003	0.207 ± 0.001	349.0 ± 0.0	–	97.8 ± 0.1
4	50	2.510 ± 0.005	0.205 ± 0.001	346.0 ± 0.7	6.2 ± 1.2	98.1 ± 0.2
Results obtained from ellipsometric measurements						
1	766	2.495 ± 0.050	0.199 ± 0.010	351.2 ± 1.5	–	–
2	52	2.519 ± 0.013	0.200 ± 0.002	346.6 ± 0.4	7.3 ± 0.2	–
3	663	2.492 ± 0.045	0.213 ± 0.009	351.3 ± 1.4	–	97.4 ± 0.6
4	10	2.521 ± 0.005	0.208 ± 0.001	346.7 ± 0.2	7.0 ± 0.1	98.4 ± 0.1

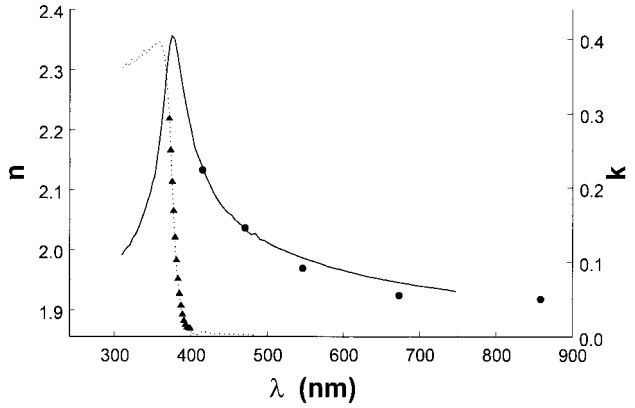

Fig. 4. Optical indices of ZnO: (●), n with direct computation; (▲), k with direct computation; (——), n with indirect computation; (····), k with indirect computation.

with spectrophotometric measurements. Spectrophotometry is therefore a good technique but not sensitive enough to microstructure parameters.

The layer thickness d_F determined by direct computation is 342.5 nm. This value is not good because the assumption of a flat homogeneous layer is not correct. However, this thickness is not too far from the thickness obtained from indirect computation methods (346.0 and 346.7 nm) and is easy to compute.

5.2. Optical indices

The optical indices of the ZnO thin film are shown in Fig. 4. It is clear that the indices depend on the assumptions made about the microstructure of the sample (flat and homogeneous for direct computation, rough and inhomogeneous for indirect computation): the curves are close but not overlaid. This is also clear from the Sellmeier parameters listed in Table 1. This proves that one must accurately determine the microstructure of a thin film before its optical indices can be calculated.

Previously published ZnO indices in the UV-visible range [34–37] have been compared with our computed indices (Table 2) to check the validity of the optical model. They all assume the ZnO to be homogeneous and flat, which is never true. Therefore, the confidence in the published ZnO indices depends on the extent of the inhomogeneity of the sample. The ZnO indices have been carefully examined. They are presented in Fig. 5. We can observe that:

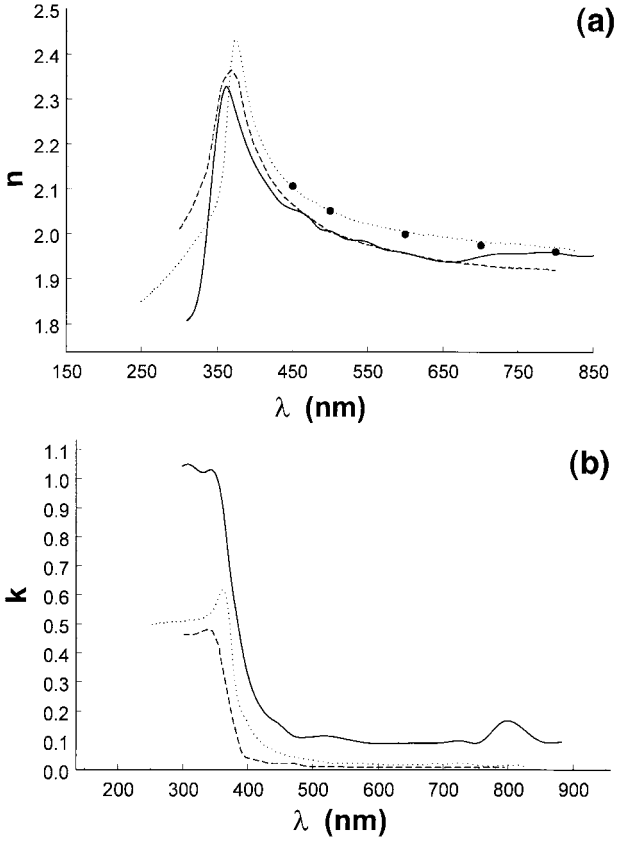

Fig. 5. Comparison between published optical indices of ZnO: (●), Bond; (——), Matz et al.; (····), Yoshikawa et al.; (– –), Koss et al.

- the n_F (λ) spectrum determined by Yoshikawa is close to that determined by Bond in the transparency domain of ZnO (ordinary index);
- the n_F (λ) values determined by Koss on a thin film are lower than those determined by Yoshikawa, which is normal because a thin film is usually less compact than a crystal;
- the n_F (λ) values determined by Matz are lower than those determined by Yoshikawa and Bond;
- the k_F (λ) values determined by Yoshikawa and Koss are close to 0 for $\lambda > 500$ nm;
- the k_F (λ) values determined by Matz are different from 0 in the visible range.

It is then concluded that the results of Yoshikawa and Bond are the best values for a ZnO crystal, that the crystal used by Matz was certainly rough or contaminated and that

Table 2
Published ZnO optical indices

Reference	Sample type	Technique	Range (nm)	Number of angles of incidence
Bond [34]	Crystal	Prism	450–800	–
Matz et al. [35]	Crystal	Nulling ellipsometry	310–810	2
Yoshikawa et al. [36]	Crystal	Ellipsometry (RAE)	250–830	1
Koss et al. [37]	film (sputtering)	Ellipsometry (RAE)	300–800	1

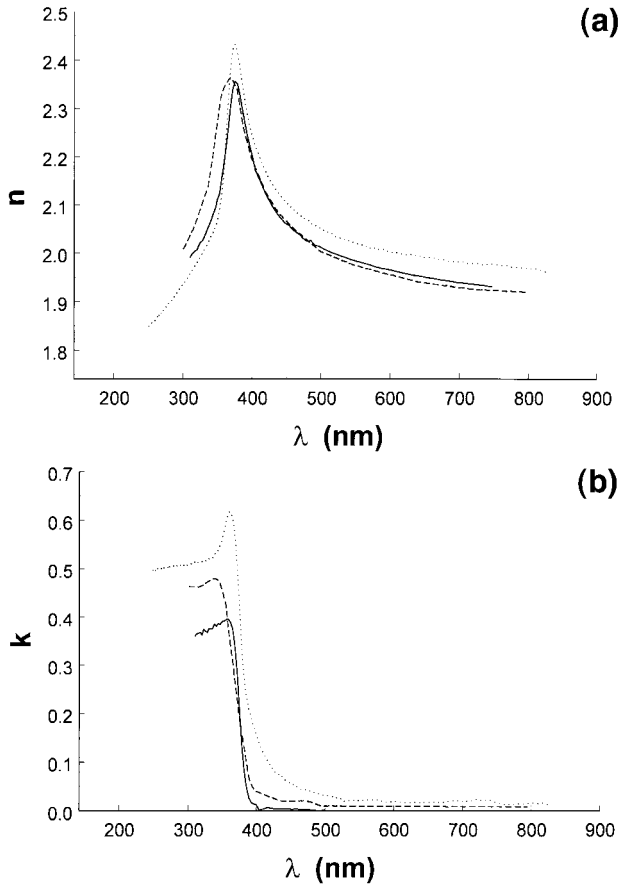

Fig. 6. Comparison between our results and published optical indices: (——), our sample; (····), Yoshikawa et al.; (– –), Koss et al.

the results of Koss are those expected for a thin film compared to that of the parent crystal. Our results were therefore compared to those of Yoshikawa and Koss (Fig. 6). It can be seen that:

- above the band gap ($\lambda > 400$ nm), the n_F (λ) values of Koss and our results are very close and are lower than the values of the ZnO crystal because of the lower density of ZnO in thin films;
- below the gap, Koss's spectrum is above that of the crystal although our spectrum is close to the values of the crystal. This difference can be explained by the fact that we first determined the structure of our sample before computing the optical indices of ZnO and Koss determined the optical indices assuming a flat homogeneous layer.

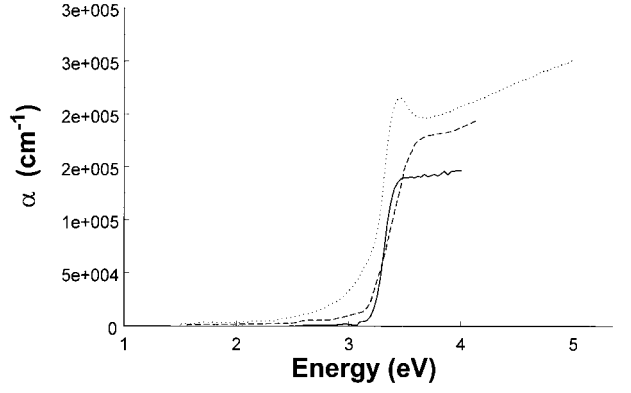

Fig. 7. Absorption features of ZnO: (——), our sample; (····), Yoshikawa et al.; (– –), Koss et al.

Table 3
Published values of the energy band gap for ZnO

Reference	Energy gap (eV)	Material
Our sample	3.27	Film, r.f. Sputtering
Yoshikawa et al. [36]	3.25	Crystal
Koss et al. [37]	3.28	Film, r.f. Sputtering
Srikant et al. [17]	3.24–3.32	Film, Laser
Gupta et al. [8]	3.23–3.31	Film, r.f. Sputtering
Heiland et al. [39]	3.20–3.43	Crystal
Tiburcio-Silver et al. [40]	3.31–3.41	Film, Pyrolysis

5.3. Band gap

The absorption coefficient of ZnO $\alpha = 4\pi k/\lambda$ has been derived from the computed k_F (λ) spectrum. In a direct gap semi-conductor, the relation between α and the energy of the incident photons is [38]

$$\alpha = \left(E - E_g\right)^{1/2} \quad (3)$$

where E_g is the energy band gap of the semi-conductor.

The $\alpha(E)$ spectrum of Yoshikawa shows the presence of an absorption exciton. Such a feature is slightly visible on Koss's spectrum. These two spectra also exhibit an absorption tail. Our sample has no exciton and has only a very weak absorption tail up to 500 nm (Fig. 7).

The curve α^2 has a linear dependance with E (Fig. 8) showing a direct transition absorption for ZnO. The energy gap for our sample is 3.27 eV. The value of E_g for our sample has been compared with published values (Table 3), and show a good agreement with these values.

6. Conclusions

We have examined the different methods used to determine simultaneously the optical indices and the microstructure parameters of a thin film with spectrophotometric and spectroscopic ellipsometry measurements. A ZnO thin film deposited on glass has been analyzed using these methods. It has been clearly shown that computed optical indices depend on the optical model used to analyse the experimental measurements. Direct computation methods with spectrophotometric measurements has been proved to give only a rough value of the thickness of the film, because the assumed microstructure for data analysis is usually not

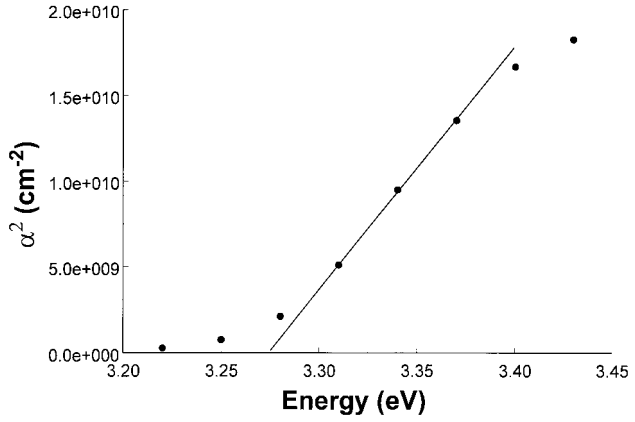

Fig. 8. Energy band gap of the ZnO sample: (●), measurements; (——), linear fit.

correct. This value is however easy to compute and can be used as a first estimation for more complex optical models. Indirect computation methods have been used with spectrophotometric and ellipsometric measurements. Although both types of measurements give the right set of values for the microstructure parameters in the best model, only ellipsometric measurements are sensitive enough to tell which model is best.

The indices n_F (λ) and k_F(λ) of ZnO were then determined in the range 310–750 nm, i.e. below and above the energy band gap. As a check of the validity of the best optical model, these were compared to previously published results and they proved to correlate closely to them.

One of the authors, Eric Dumont, acknowledges the support of a grant from the FRIA (Fonds pour la formation à la recherche dans l'industrie et dans l'agriculture).

References

[1] H.L. Hartnagel, A.L. Dawar, A.K. Jain, C. Jagadish, Semiconducting Transparent Thin Films, Institute of Physics Publishing, Bristol, 1995.
[2] C.G. Granqvist, Thin Solid Films 193-194 (1990) 730.
[3] Z.C. Jin, I. Hamberg, C.G. Granqvist, Thin Solid Films 164 (1988) 381.
[4] A. Banerjee, D. Wolf, J. Yang, S. Guha, J. Appl. Phys. 70 (1991) 1692.
[5] H. Herrmann, K. Schäfer, W. Sohler, Photonics Technol. Lett. 6 (1994) 1335.
[6] G.J. Exarhos, S.K. Sharma, Thin Solid Films 270 (1995) 27.
[7] B. Szyszka, S. Jäger, J. Non-Cryst. Solids 218 (1997) 74.
[8] V. Gupta, A. Mansingh, J. Appl. Phys. 80 (1996) 1063.
[9] R. Wang, L.L.H. King, A.W. Sleight, J. Mater. Res. 11 (1996) 1659.
[10] S.H. Hayamizu, H. Tabata, H. Tanaka, T. Kawai, J. Appl. Phys. 80 (1996) 787.
[11] G. Exarhos, L.Q. Wang, T. Dennis, Thin Solid Films 253 (1994) 41.
[12] W.W. Wenas, A. Yamada, K. Takahashi, M. Yoshino, M. Konagai, J. Appl. Phys. 70 (1991) 7119.
[13] M.O. Abou-Helal, W.T. Seeber, J. Non-Cryst. Solids 218 (1997) 139.
[14] C.R. Aita, A.J. Purdes, R.J. Lad, P.D. Funkenbusch, J. Appl. Phys. 51 (1980) 5533.
[15] C.R. Aita, R.J. Lad, J. Appl. Phys. 51 (1980) 6405.
[16] H. Nanto, T. Minami, S. Shooji, S. Takata, J. Appl. Phys. 55 (1984) 1029.
[17] V. Srikant, D.R. Clarke, J. Appl. Phys. 81 (1997) 6357.
[18] C.J. Gawlak, C.R. Aita, J. Vac. Sci. Technol. A 1 (1983) 415.
[19] P. Chindaudom, K. Vedam, Characterization of inhomogeneous transparent films, Physics of Thin Films, Vol. 19, Academic Press, New York, 1994, pp. 191–247.
[20] S. Bertucci, A. Pawlowski, N. Nicolas, L. Johann, A. El, Ghemmaz, N. Stein, R. Klein, Thin Solid Films 313-314 (1998) 73.
[21] U. Richter, Thin Solid Films 313-314 (1998) 102.
[22] J.C. Manifacier, J. Gasiot, J.P. Fillard, J. Phys. E 9 (1976) 1002.
[23] P. Swanepoel, J. Phys. E 16 (1983) 1214.
[24] J.P. Borgogno, B. Lazarides, E. Pelletier, Appl. Opt. 21 (1982)4020.
[25] R.M.A. Azzam, N.M. Bashara, Ellipsometry and Polarized Light, North Holland, Amsterdam, 1977.
[26] G.E. Jellison Jr, Thin Solid Films 313-314 (1998) 33.
[27] J.J. Moré, in: G.A. Watson (Ed.), Lecture Notes in Mathematics, Vol. 630, Springer, Berlin, 1978.
[28] W.A. McGahan, B. Johs, J.A. Woollam, Thin Solid Films 234 (1993) 443.
[29] G.E. Jellison, F.A. Modine, Appl. Phys. Lett. 69 (1996) 371.
[30] G.E. Jellison, F.A. Modine, Appl. Phys. Lett. 69 (1996) 2137.
[31] B. Tatian, Appl. Opt. 23 (1984) 4477.
[32] J. Ph, J. Roussel, H.E. Vanhellemont, Maes, Thin Solid Films 234 (1993) 423.
[33] D.E. Aspnes, J.B. Theeten, F. Hottier, Physical Rev. B 20 (1979) 3292.
[34] W.L. Bond, J. Appl. Phys. 36 (1965) 1674.
[35] R. Matz, H. Lütz, Appl. Phys. 18 (1979) 123.
[36] H. Yoshikawa, S. Adachi, Jpn. J. Appl. Phys. 36 (1997) 6237.
[37] V. Koss, A. Belkind, K. Memarzadeh, J.A. Woollam, Sol. Energy Mater. 19 (1989) 67.
[38] T.S. Moss, Optical Properties of Semiconductors, Butterwooths Scientific Publications, London, 1959.
[39] G. Heiland, E. Mollwo, F. Stockmann, Solid State Phys. 8 (1959) 191.
[40] A. Tiburcio-Silver, J.C. Joubert, M. Labeau, J. Appl. Phys. 76 (1994) 1992.